Desalination and Water Treatment
www.deswater.com

doi:10.5004/dwt.2019.24254

166 (2019) 168–179
October

Fusion rules and image enhancement of unmanned aerial vehicle remote sensing imagery for ecological canal data extraction

Zichao Zhang[a,b,#], Yu Han[c,#], Jian Chen[a,b,d,e,*], Yi Cao[a], Shubo Wang[a], Guangqi Wang[a], Nannan Du[a]

[a]*College of Engineering, China Agricultural University, 17 Qinghua East Rd., Beijing 100083, China, email: zhangzc1@cau.edu.cn (Z. Zhang), Tel. 86–18810922501, email: jchen@cau.edu.cn (J. Chen), Caoyi@cau.edu.cn (Y. Cao), wangshubo@cau.edu.cn (S. Wang), wangguangqi@cau.edu.cn (G. Wang), dnngxy@cau.edu.cn (N. Du)*
[b]*Synergistic Innovation Center of Jiangsu Modern Agricultural Equipment and Technology, Jiangsu University, 301 Xuefu Rd., Zhenjiang 212013, China*
[c]*College of Water Resources & Civil Engineering, China Agricultural University, 17 Qinghua East Rd., Beijing 100083, China, email: yhan@cau.edu.cn (Y. Han)*
[d]*State Key Laboratory of Information Engineering in Surveying, Mapping and Remote Sensing, Wuhan University, 129 Luoyu Rd., Wuhan 430079, China*
[e]*Beijing Key Laboratory of Optimized Design for Modern Agricultural Equipment, China Agricultural University,17 Qinghua East Rd., Beijing 100083, China*

Received 27 July 2018; Accepted 19 February 2019

ABSTRACT

For the problem of rough irrigation habits and low irrigation efficiency in Hetao irrigation area in China, which only pays attention to increasing yield, this paper proposes a method of accurate extraction of canal information based on fusion of rules and image enhancement in order to improve the level of canal irrigation management in Hetao irrigation area. Accurate calibration of canal information is the premise of precision irrigation management. For satellite remote sensing, it is difficult to collect information with high accuracy in sub lateral ditches in the field. For ground stations, calibration work is difficult to move flexibly with the target. Therefore, based on UAV remote sensing images and object-oriented segmentation method, a fusion of rules of two spectral features and two shape features was adopted. The optimal combination rule of "image enhancement splicing threshold 2%, normalized chromatic aberration coefficient a = 0.1, b = 0.9, c = 1.2, spectral average less than 98, minimum enclosure rectangle aspect ratio between its minimum value and 1, extension line greater than 1 meter" was obtained. The information of some ecological canal system in Hetao Irrigation District of Inner Mongolia was extracted, and the recognition accuracy reached sub lateral ditches level. The two evaluation methods of canal system calibration were put forward and the experiment was evaluated. The correct rate of sample 1 interpretation of combination rules was 87.5%, SNR (Signal-to-Noise Ratio) of classification results was 7.602, which provided accurate canal system information for precise irrigation operation and management.

Keywords: Precision irrigation; Hetao irrigation area; Ecological canal system; UAV remote sensing image; Image segmentation; Feature extraction.

1. Introduction

Precision irrigation technology is a systematic project, which is based on the integration of multiple information technology platforms and various agricultural technologies in 21st century [1,2]. The precision irrigation technology is based on the big field tillage. According to the requirements of the crop growth process, the results are obtained by modern testing methods, and the most accurate irrigation facilities are used to fertilize the crop radially with high efficiency [3,4]. In order to increase yield, the single focus on the expansion of planting area and the rough irrigation tradition made the ecology of Hetao irrigation area very fragile for a time [5,6]. As an import-

*Corresponding author.

ant part of precision agriculture, precision irrigation improves the irrigation efficiency of self–flowing irrigation area by leaps and bounds [7]. Xue and Ren [8] analyzed and evaluated the agricultural hydrological model of Hetao Irrigation District in Inner Mongolia. It was concluded that the improvement of irrigation management could improve the productivity of Hetao Irrigation District and save groundwater, which had been decreasing gradually in recent ten years. However, the article only gives a brief description of the canal system and gives a basic overview of the canal system in Hetao irrigation area, and the canal system management is very important in groundwater management. Wang et al. [9] described in detail the construction and operation management of farmland drainage ditch and pond wetland system in ecological irrigation area, pointed out the importance of drainage ditch and pond system for ecological irrigation area, divided the scale of farmland drainage ditch and pond system, and pointed out the importance of farmland drainage ditch and pond system operation and management. The operation and management methods described above were comprehensive, and the economic output per unit water volume of irrigation water management was analyzed with multi-factors. However, the combination with technical level was less, and there was no more description of information extraction and improvement. The practical application needed further study and discussion. The artificial and natural composite surface water system in Hetao irrigation area is the most important and positive factor in the regional water cycle [10,11]. This means that in the modern ecological construction of Hetao irrigation area, attention should be paid not only to the technical aspects of precision irrigation, but also to the management methods.

The premise of water use management and canal system dispatching management is information management, and the calibration of precise geographic information coordinates of field furrows and buckets is the key factor to obtain information of ecological canal system [12,13]. In general, calibration of such geographic information (sub lateral ditches level) is carried out with carrier calibration and manual calibration. For large irrigation districts such as Hetao irrigation area, there are limitations in calibration and manual calibration. The calibration of ground vehicles will not only damage farmland and its crops, but also require high performance of ground vehicles. The manual calibration efficiency and its inefficiency are extremely unsuitable for such a field farming environment as Hetao Irrigation District. Compared with the above two calibration methods, UAV, as a remote sensing platform, is not restricted by working environment in all kinds of applications except extreme weather [14–18]. Gago et al. [19] improved the level of irrigation management by using UAV remote sensing platform and various spectral information vegetation evaluation indicators. In the concept of precision agriculture, remote sensing technology can provide observation data with high timeliness, coverage and objectivity, and can improve the level of agricultural detection system [20,21]. Commonly used remote sensing platforms include satellites, UAVs and ground stations. Generally, the resolution of civil satellite remote sensing is not enough to complete the agricultural statistics work which needs high-resolution remote sensing data in precision agriculture, such as the identification of sub lateral ditches, and the need of 0.1 m or higher-precision remote sensing data [22–24]. The ground station has the highest resolution of remote sensing, but its high construction cost is too difficult to popularize. The advantages of UAV remote sensing technology are: compared with satellite remote sensing, UAV remote sensing is less affected by clouds; low-altitude flight greatly improves resolution; strong emergency response capability, and high efficiency on duty. These advantages have great potential for the application of UAV remote sensing technology in agriculture [25,26].

As we all know, feature extraction is a systemic problem. An extraction object usually has many features in a dataset [27,28]. For target extraction and extraction problems, high resolution images do not have advantages in pixel-level classification [29–32]. High resolution data, including image data, radar data, etc., where one or a few pixels or a few units of information usually do not fully express an extraction element [33–35]. The extraction of information, and a real-world object cannot be described clearly by a single pixel value [36]. Thus, dividing the original data into objects can greatly reduce the computational complexity of high-resolution data in data processing [37,38]. And in the process of object segmentation, it is possible to eliminate partial noise in the data [39]. For object-oriented remote sensing data, we can adjust the scale of segmentation to process as much as possible a unit belonging to an object in space as an object has been achieved in many studies. Jozdani et al. [40] introduced the work of extracting buildings from remote sensing data through multi-scale segmentation and subsequent processing, but for this study, the characteristics of buildings and canals are very different, and the environment is different, so the reference is poor. The method presented in [41] can solve the problem of information loss of high-resolution remote sensing data very well, but the scale of farmland remote sensing data described in this paper is different from that in this study. The information of ecological canal system in some irrigation areas is supplemented in this paper, but it is not very helpful to the information of sub lateral ditches level. Refs. [42–44] is suitable for segmentation of required features. In view of the features that need to be extracted in this research, the application of multi-scale segmentation in high-resolution remote sensing data is necessary.

Therefore, fusion of rules method can greatly improve the extraction accuracy and SNR of feature extraction results. Canal system features can be described by many rules, but the description of single feature rule is not enough to extract canal system from remote sensing image data. Aiming at the artificial-natural compound surface water system in the ecological canal system construction project of Hetao Irrigation District, in order to improve the management level of irrigation water, the UAV remote sensing technology is used. Some remote sensing image data collected by UAV was fused with object-oriented segmentation method, two spectral-feature rules and two shape feature rules. The distribution information of farmland ecological canal system in irrigation area was extracted, and the evaluation indexes of accuracy rate based on distance and SRN based on classification results were put forward. Combined with the geographic information obtained by UAV, the precise coordinates of farmland ecological canal system in irrigation area can be obtained, which can provide accurate reference data for the next precise irrigation diversion work.

2. Data and methods

The total area of Inner Mongolia Hetao irrigation area is 112×10^3 km^2, the irrigation area of the river diversion

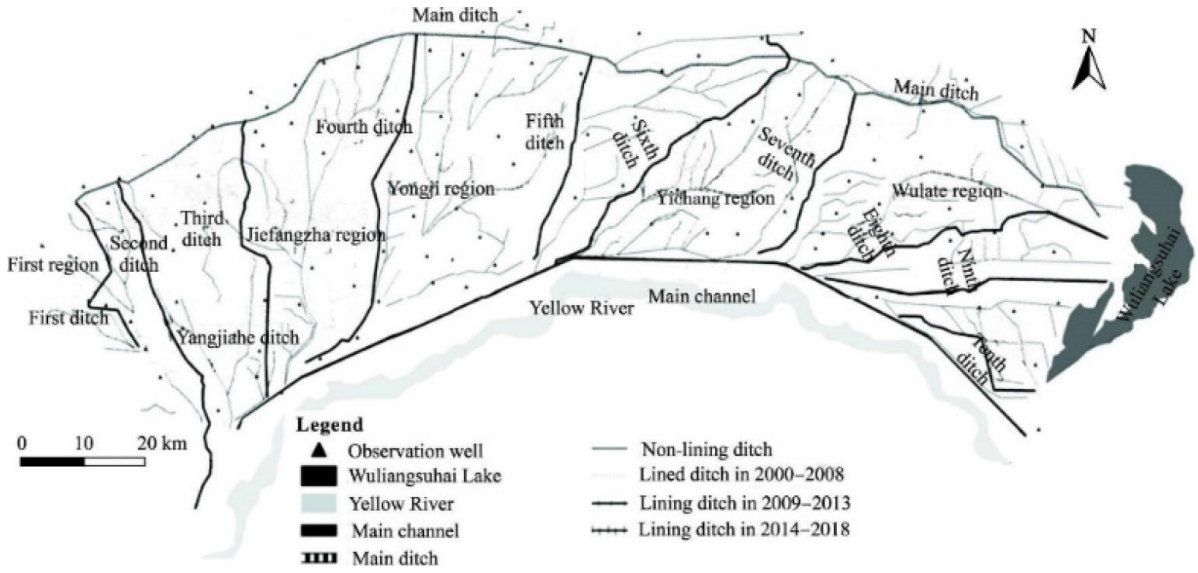

Fig. 1. General situation of canal system in Hetao irrigation area.

river reaches 57.4 × 10^3 km^2 , the annual water quantity of the Yellow River is about 50 × 10^8 m^3, as shown in Fig. 1. The main channel (180 km) through the west to the east through the various levels, the water supply of the main canal, and the irrigation and retreat of the farmland into the main ditch (220 km) in the northern part of the irrigation area through the main gully at all levels. The main channel, the main ditch, and main gully have lining treatments. Therefore, under the extensive irrigation conditions, the waste of the sub lateral ditches is the main reason for the low irrigation efficiency in the irrigation area.

2.1. Remote sensing image data pre-processing

Image pre-processing is the first step in image segmentation. In remote sensing data, taking UAV remote sensing image as an example, the acquisition of remote sensing data is easily disturbed by weather, such as fog and haze. If the image is disturbed, and the features of remote sensing data are not easily identified in the original image, the threshold of remote sensing image processing is difficult to be segmented, and the difficulty of the further classification of remote sensing images is further increased.

The processing method of linear drawing is the same as that of gray scale drawing transformation:

$$Data' = \begin{cases} 0 & 0 \le Data \le A \\ \frac{255}{B-A}(Data-A) & A \le Data \le B \\ 255 & B \le Data \le 255 \end{cases} \quad (1)$$

where *Data* and *Data´* represent the gray value of the input image, and the output image respectively. After linear transformation, the gray value between A and B is stretched, and the interval less than A and B is suppressed. In the same way, for the RGB image, the decomposition RGB model color image is 3 color channels, and the pixel gray value-based operation on the decomposed 3 color channels is enhanced respectively. Finally, the enhanced 3 channels are synthesized into new color images. Take the R channel as an example:

$$RData' = k\frac{RData-Min}{Max-Min} \quad (2)$$

where *RData* is the value of the input R channel pixels, *RData'* is the value of the output R channel piexls. This method is very good for the enhancement of the middle area, which is very suitable for the remote sensing image data of UAV. In this paper, the linear drawing of color image is applied to the images which are difficult to be segmented by the threshold, or the original image is photographed in the dark environment. Experimental results are shown in Fig. 2.

As shown in Fig. 2, first, the threshold of linear stretching is set to 2%, linear cutting stretching is based on the limits of 2% and 98%. The values of the nearest distribution are selected as the range of tensile data respectively. As shown in the above picture, the RGB image is shown in the R channel, and the two ends of the dotted lines are 2% and 98% in the upper drawing as A and B in Eq. (1), and the data in the two thresholds are intercepted into the new graph. Linear stretching, as shown on the right, the histogram distribution in the histogram of R channel is more average than that in the left map, and the same G and B band data are even more uniform than before.

2.2. Image segmentation based on object-oriented method

In the development of geographic information system image classification, the resolution of high-resolution remote sensing data is increased, but the classification method based on pixel, such as the classification based on the spectrum and the classification based on the decision tree, has low resolution and an increase in the error. The object-oriented classification divides the remote sensing data into multiple objects, and classifies the object based on the segmentation object, which makes the work efficiency and resolution precision greatly increased as shown in Fig. 3. Furthermore, different methods can get different results.

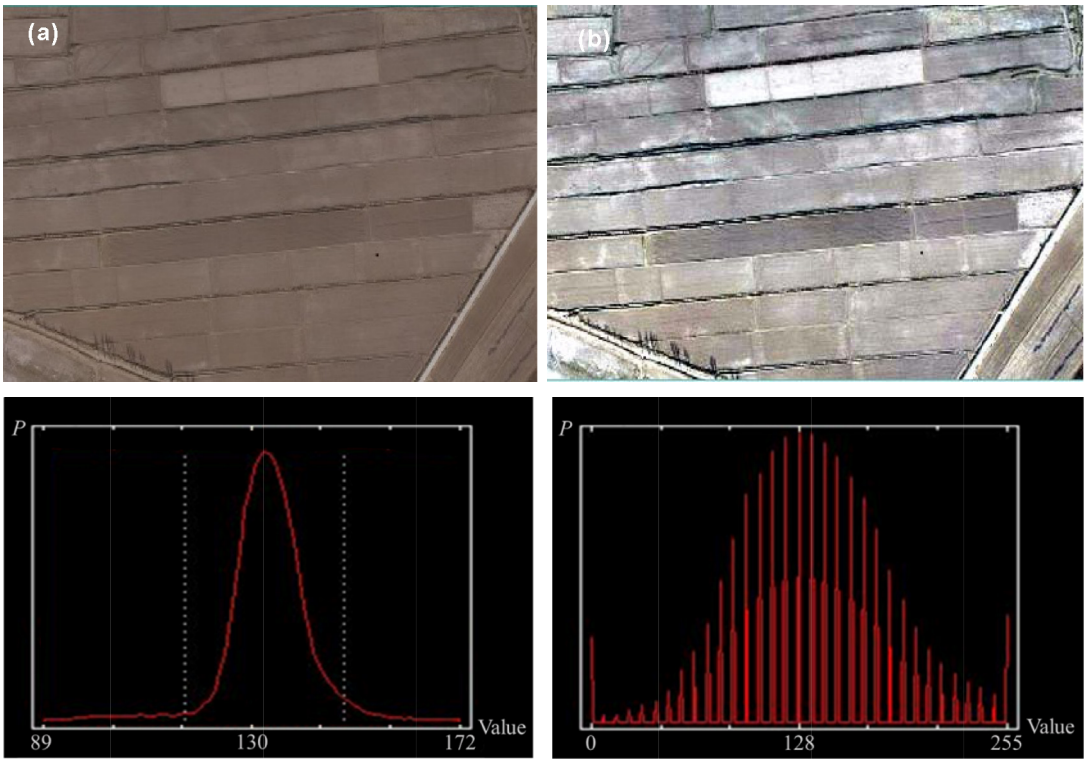

Fig. 2. Linear stretching (as an example of R channel), A is the original map of the canal system, B is a stretched figure, the original histogram of R channel is C, and D is the stretched histogram of R channel.

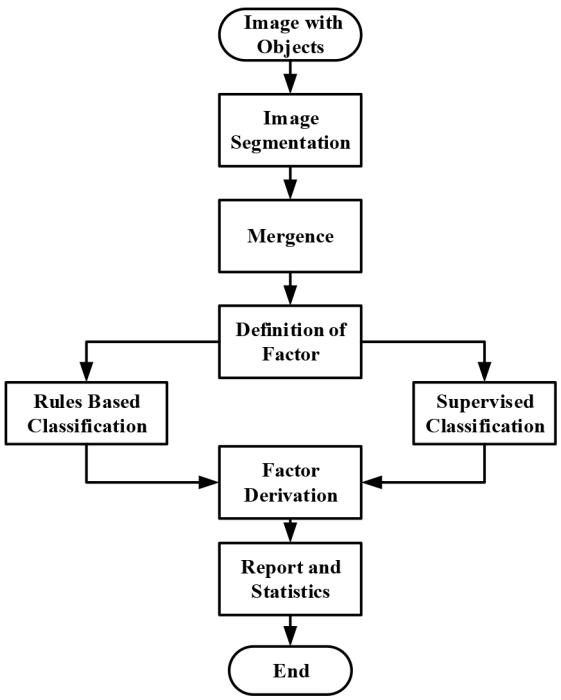

Fig. 3. Technical route of object-oriented image segmentation.

Image segmentation is the first step and the most crucial step of object-oriented method. The selection of the segmentation threshold directly determines the accuracy of the object-oriented image segmentation. The selection of the high-scale image segmentation-threshold will separate the few spots, so the segmentation greatly eliminates the noise caused by the image stretching, but the useful information which is needed will be eliminated. The selection of a low scale image segmentation threshold will divide more objects with the richer information, but the segmentation effect affects the accuracy of the classification effect. The other threshold provided by ENVI 5.1 is the combination threshold, which combines the segmentation image further. To a certain extent, it can eliminate the noise generated by the segmentation threshold, and other noises are eliminated in the regular classification, but the high resolution cannot reach the requirement of the resolution.

In view of the remote sensing image data collected, the segmentation threshold can be set low because of its high resolution, which can make it 40; there are many sundries in the field. It is necessary to remove a part of the field in the merged part, so that every field should be treated as an object as far as possible, and the choice of the combination threshold of this paper is 95. The processing results are shown in Fig. 4.

2.3. Definition of factor based on rule classification

In defining the factor stage, the definition elements of object-oriented classification are classified into rule-based classification and supervised classification. Rule classification is composed of several rules in each classification, and each rule has several attribute expressions to describe. Attribute expressions correlate with other attribute expres-

Fig. 4. Object oriented segmentation results.

sion as sum aggregate, Rules correlate with other rules as intersection. The same kind of ground objects can be described by different rules. In remote sensing images, such as water bodies, and the water bodies can be artificial ponds, lakes, rivers, and natural lakes and rivers. The rules are different, and many rules are needed to describe each rule, and each rule has several attributes. The classification based on supervision is to manually interpret and select representative objects on the basis of the objects that have been divided, and the computer automatically adjusts the rules according to the selected samples. The classification based on supervision is divided into K Nearest Neighbor, Support Vector Machine (SVM), and Principal Components Analysis (PCA).

The supervised classification, the more samples are selected manually, the more the object samples are selected and the more the samples are distributed in the graph, the more accurate the classification results will be, and the accuracy can be close to the artificial interpretation accuracy in the ideal state. But for the object of this paper, the noise of remote sensing data has a great influence on the supervised classification, and the actual classification results are noisier. It requires a huge amount of manual interpretation and correction, and the selection of the objects of different remote sensing data is different, so, the adaptability of the remote sensing data with the same features is poor. Based on the definition of the factor of supervision, compared with the definition of rule-based elements, the extraction efficiency of sub lateral ditches in large irrigation area is low.

Therefore, this research chooses the rule-based classification method in the definition stage of this investigation. The remote sensing data collected in this work are carried out in winter, and the sub lateral ditches in the field are all in the dry state. The difference between the spectral information and other objects is mainly in the shadow caused by the sun being blocked by the boundary of the canal system when the image is filmed. Its shadow features are not controlled by many factors, and sublateral ditches are the most easily damaged canal system during fallow period. The main gully is basically reformed, the bottom and the hardening, as the main water system in the irrigation area, are more protected, and the external factors such as the width of the ditch and the ditch are easy to identify in the remote sensing recognition. On the contrary, due to the direct connection with the irrigated field, the field production will affect its integrity to varying degrees. This paper also makes a comparison of its features, and makes an artificial interpretation (Ground Truth) based on the segmentation results and the definition of elements, and compares the results with those of the correct interpretation.

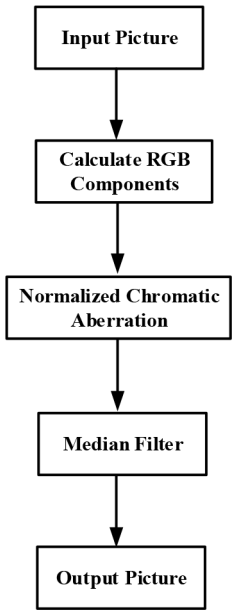

Fig. 5. Processing flow of normalized chromatic aberration.

3. Experimental results and analysis

3.1. Classification with spectral mean value rules

Firstly, spectral mean value rule is used to classify objects. According to the shadow information, the shadow of the field canals is obvious, so when the spectral average is used to classify the information, the information is retained as the shadow information, and the spectral information with a smaller average value is retained. Generally speaking, the area of canal system in remote sensing images is small, so its texture scale is small as well. Because of the occlusion of the boundary of canal system, the gray level is not smooth, and the shadow area exists. Using this characteristic, the spectral average rule is selected to classify the objects. The rule of spectral average first uses the spectral characteristics of each remote sensing pixel data of UAV to get the average value of each object block, and then uses the average value of the obtained spectrum to calculate and classify:

$$d = \frac{\sum_{i=1}^{R}\sum_{j=1}^{C} DN(i,j)}{R \times C} \tag{3}$$

where d is the average spectral value, i is the number of rows of pixels, J is the number of columns of pixels, $N_{(i,j)}$ is the spectral curve of the pixel in the i row and the J column. When $d > 98$, shadows were deleted, when $d > 98$, the shadows were kept. When using spectral average to classify, the spectral average value of each pixel in the image is calcu-

lated according to Eq. (3), and the spectral map is obtained. The information is extracted by setting a reasonable threshold according to the spectrogram.

The spectral mean threshold is manually debugged and the average value of the spectrum is less than 98, as shown in Fig. 7A. At the same time, the artificial interpretation comparison based on the extraction results will also be given under the result diagram

3.2. Classification with shape rules

In the classification of object elements, the classification of objects based on the shape is a typical kind of classification method. The limit conditions of the object are round degree, the smallest ratio of rectangle length to width ratio and so on. When the object is used to classify the shape rules, the shape information of the extracted object elements needs different shape information relative to the surrounding objects. For the objects such as sub lateral ditches in the field, the ratio of the length to the width has obvious characteristics relative to other objects, and its aspect ratio is far greater than 1. The result of manual interpretation based on the result of shape rule classification is also shown below:

$$P = \frac{l_{\max}}{l_{\min}} \tag{4}$$

where P is aspect ratio of the minimum enclosing rectangle, l_{min} and l_{max} are the width and length of the minimum enclosing rectangle, respectively. When $P > 1$, the objects were kept, when $P \leq 1$, the objects were deleted.

3.3. Classification with the extension line

According to the extraction method of the extension line, the features of the geographical information with linear feature and the feature of the object lengthening are more prominent, such as mountain rivers, etc. The extraction of ecological canal system in this paper also has good directional characteristics, so it is feasible to use ecological characteristics of extension line to extract ecological canal system

$$G = \max\{L;W;C\} \tag{5}$$

where G is the selected extension line in three elements in objects. L is the biggest side length in objects, W is the biggest side width and C is the longest diagonal or cross line in objects.

3.4. Classification with normalized chromatic aberration

Due to the difference in color between the canal and the field and the road, the canal area in the image can be extracted by using the color characteristics of the canal system. Part of the current image segmentation research is based on color image segmentation algorithm research. The selection of color space is first required before color image segmentation. This paper chose the RGB color space. Because color images mostly use color space, in order to make the color difference between the canal and the field more obvious, in order to more effectively segment the channel region in the image, it is necessary to select a color space to display a more obvious color. The color of this experimental image is more distinct in the RGB space. After the color space is determined, one or several initial color components in the color space are directly used as color features to distinguish the color difference between the canal and the field. Then based on the color feature, the image segmentation algorithm is designed to realize the segmentation between the canal and the field. The initial color of color space is used as the color feature for image segmentation. Because its principle is simple and its modeling work is not complicated, so the segmentation speed is fast and the real-time performance is good. In this paper, we choose the image segmentation algorithm based on normalized color difference, mainly by calculating the values of three components R, G, and B to realize the extraction of the canal system. The calculation formula of normalized color difference:

$$S = \frac{a \times R + b \times B}{c \times (R + G + B)} \tag{6}$$

where $a + b = 1$, $a \in (0,1)$, $b \in (0,1)$ and $c \in (0,2)$. S is normalized chromatic aberration, R, G, B, is the red, green and blue channel of the color image. For the color characteristics of canal system, we set $a = 0.1$, $b = 0.9$, $c = 1.2$. The processing flow is as Fig. 6.

3.5. Classification with combinatorial extraction

Direct combination of rules extraction is destructive to feature description, so this paper fine-tuning the description features. In this paper, the information of the ecological canal system is as follows: the spectral mean value is less than 98, the minimum bounding rectangle length width

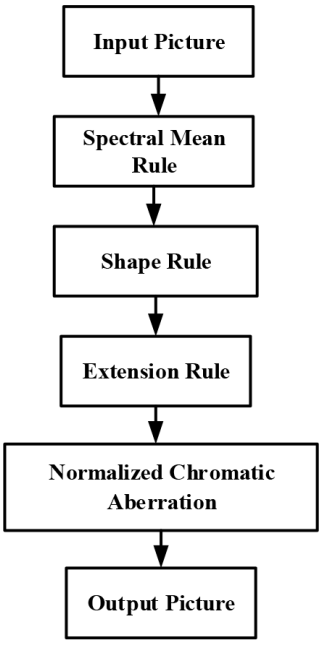

Fig. 6. Processing flow of combinatorial extraction.

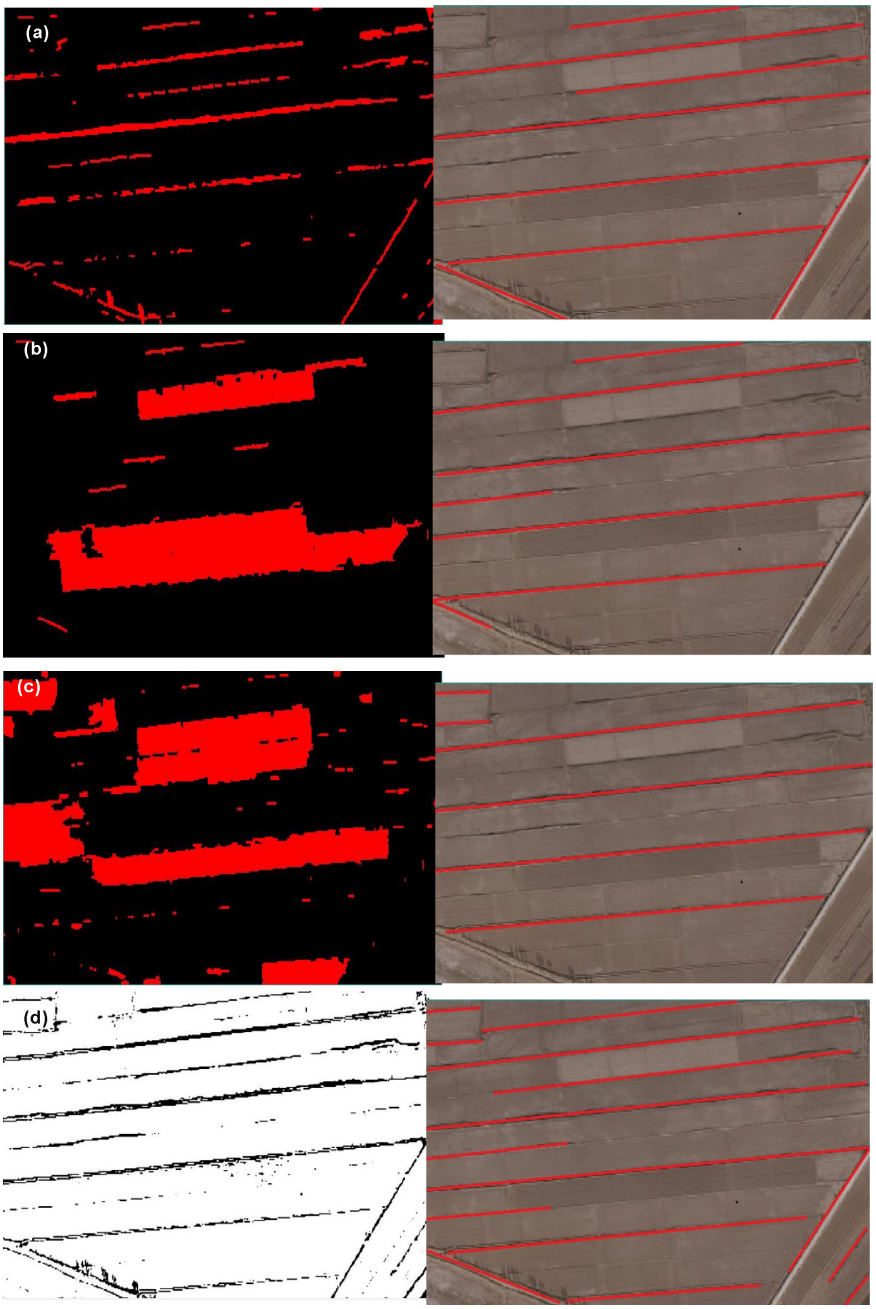

Fig. 7. Four sets of rule-based results and interpretations of sample 1. A is classification with spectral mean value rules, B is classification based on shape rules, C is classification with extension line, D is classification with the normalized chromatic aberration.

ratio is between the minimum and 0.85, and the lengthening line is more than 1 m. The extraction results were as follows. The manual interpretation based on information extraction is shown in Fig. 7D.

3.6. Evaluation of experimental results

The methods of geographic information classification technology tend to be improved. Many automatic classification techniques emerge in an endless stream. In the ideal situation, the classification of geographic information can be classified in a short time, and the accuracy is close to the accuracy achieved by artificial interpretation. However, the highest and most reliable classification method of the highest precision is still artificial interpretation. In this paper, we manually interpret four sets of categorical data, as shown in Fig. 7. Relative accuracy of manual interpretation results has been given, and the accuracy of evaluation indicators is given:

$$p = \frac{L - \sum_{1}^{m} |errors|}{L} \times 100\% \tag{7}$$

where $L = 12\ km$ is known length of sub lateral ditches in our sample. The *errors* is the length of the mistranslation or leakage of the sub lateral ditches in various classifications, in which the *errors* is positive when mistranslated, and the *errors* is negative in the missed translation m is the number of missing or mistranslation of sub lateral ditches. According to the above evaluation index, the results of this paper were shown in Table 1.

The comparison between Fig. 7, Fig. 8 and Table 1 can be summed up as follows: First, the auxiliary interpretation assistance based on the definition of the elements of the three rules can promote the efficiency of manual interpretation, the accuracy rate is also higher than any single rule. Second, the result of the auxiliary interpretation based on the definition of the shape rule is inaccurate, and the information obtained by the definition of the element is more information of the ridge than the ecological canal system, the higher accurate of auxiliary interpretation result in image enhancement caused by overlap display, but it lacks with actual reference value. It has no positive effect on further research based on non-artificial interpretation, such as artificial intelligence classification technology. Third, only based on the definition of spectral mean factors, rules interpretation is more likely to be misinterpreted, such as the translation of ridge of field into an ecological canal system.

Aiming at the problem that the evaluation effect of correct probability of information acquisition and interpretation in KM unit is not good, we propose another evaluation index of correct rate in pixel unit, which is pixel signal-to-noise ratio:

$$SNR = \frac{Z_g}{Ze} \tag{8}$$

where SNR is defined as the signal-to-noise ratio of ditch pixels in the selected area, Z_g is the number of ditch pixels, Z_e is the number of noise pixels such as ridges and roads.

Through comparison, it is found that the signal-to-noise ratio of canal system extracted by normalized chromatic aberration and spectral average method is higher; the area extracted by extended line rule has larger field area and lower signal-to-noise ratio; the area extracted by shape rule has larger road and field area and the signal-to-noise ratio is the lowest; the normalized chromatic aberration, spectral average rule and spectral average rule are used. The combination of shape rule and extension line rule achieves a good extraction of ditches, with the highest signal-to-noise ratio and the basic noise filtering of fields and roads. The results were shown in Table 3 and Table 4.

Table 1
Result of different extraction of sample 1

	Ground truth	Spectral mean value rule	Shape rule	The extension line rule	Normalized chromatic aberration rule	Combinatorial extraction
Interpretation of length L/km	12	14.5	10	8	18	13
$\sum_{1}^{m}\lvert errors\rvert$	0	2.5	2.5	2	5	1.5
Missing or mistranslation number	0	2	4	2	5	2
Correct rate	100%	79.2%	75.0%	80.0%	50.0%	87.5%

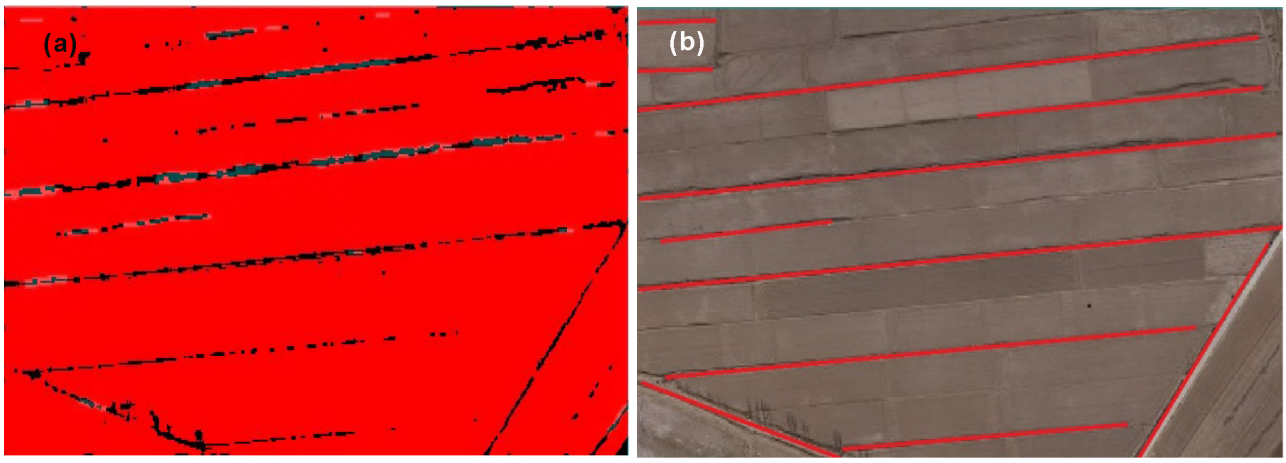

Fig. 8. Combinatorial extraction results (left) and interpretations of sample 2.

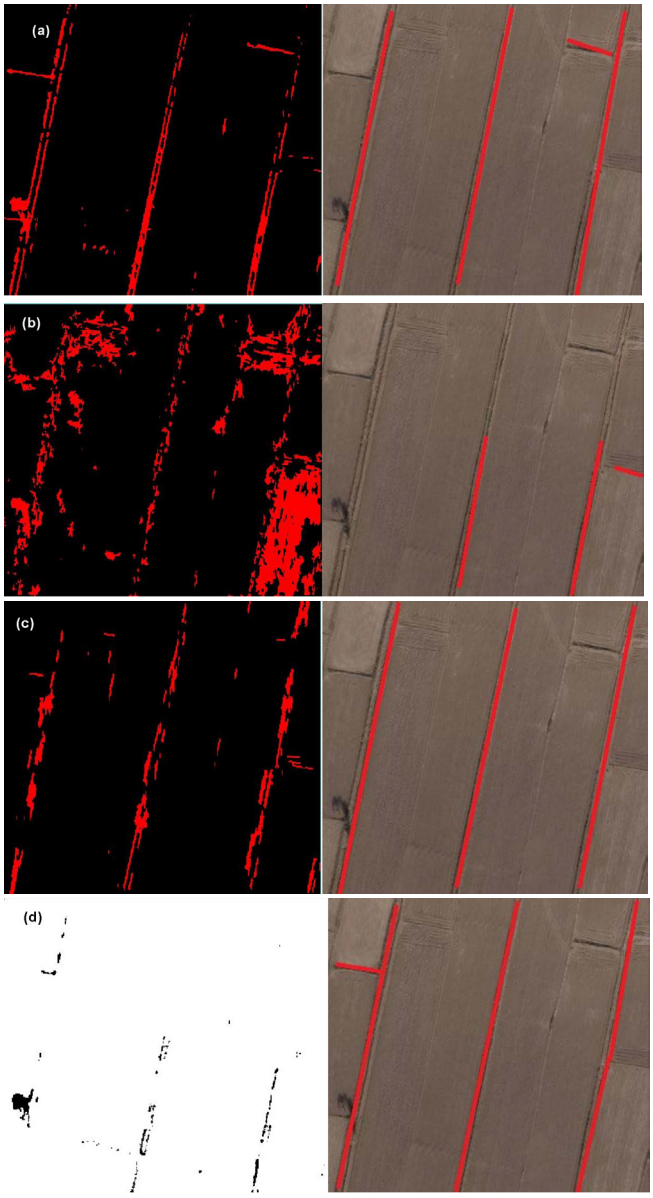

Fig. 9. Four sets of rule-based results and interpretations of sample 2. A is Classification with spectral mean value rules, B is classification based on shape rules, C is classification with extension line, D is classification with the normalized chromatic aberration.

Table 2
Result of different extraction of sample 2

	Ground truth	Spectral mean value rule	Shape rule	The extension line rule	Normalized chromatic aberration rule	Combinatorial extraction
Interpretation of length L/km	6	6.5	3	6	6.5	5.5
$\sum_{1}^{m}\lvert errors\rvert$	0	0.5	4	0	0.5	0.5
Missing or mistranslation number	0	1	2	0	1	2
Correct rate	100%	90%	33.3%	100%	90%	90%

Table 3
SNR of different extraction of sample 1

	Spectral mean value rule	Shape rule	Extension line	Normalized chromatic aberration rule	Combinatorial extraction
Number of ditch pixels	710	420	598	2080	1684
Number of noise pixels	242	1460	1846	1530	221
Signal to noise ratio	2.934	0.014	0.324	1.359	7.602

Table 4
SNR of different extraction of sample 2

	Spectral mean value rule	Shape rule	Extension line	Normalized chromatic aberration rule	Combinatorial extraction
Number of ditch pixels	550	356	412	1632	1375
Number of noise pixels	158	986	846	1330	147
Signal to noise ratio	3.481	0.361	0.487	1.227	9.354

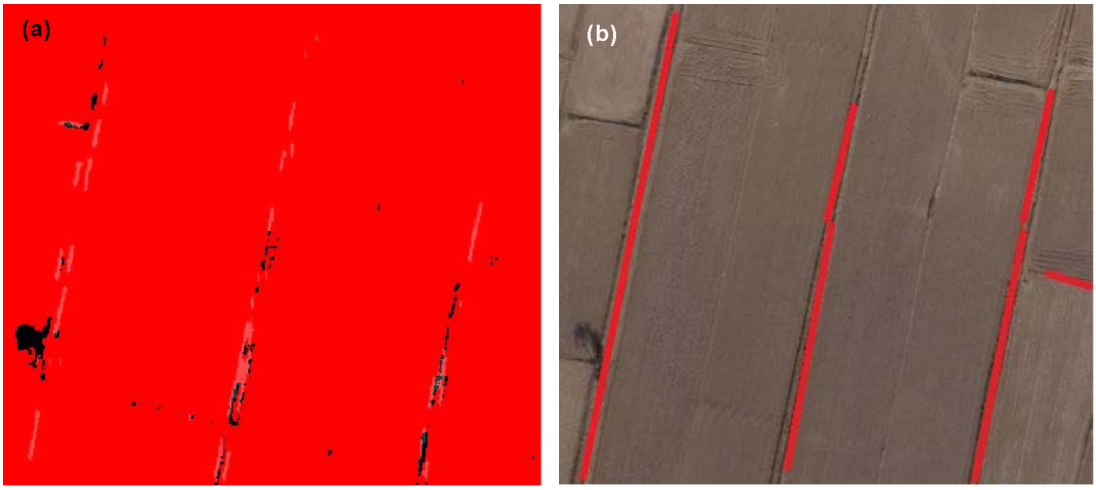

Fig. 10. Combinatorial extraction results (left) and interpretations of sample 2.

4. Conclusions

In this work, some remote sensing image data collected by UAV are processed by ENVI 5.1, and the optimal combination rule of "image enhancement splicing threshold 2%, normalized chromatic aberration coefficient a = 0.1, b = 0.9, c 1.2, spectral average less than 98, minimum enclosure rectangle aspect ratio between its minimum value and 1, extension line greater than 1 meter" is obtained. Based on the combination rule, the distribution information of ecological canal system in ecological irrigation area was extracted. The two-evaluation index was given, and the result of the auxiliary interpretation was compared with the correct interpretation result, and the result of the optimal combination rule was 87.5%, SNR (Signal-to-Noise Ratio) of classification results was 7.602. The next research will combine the information of the canal system with the information of the UAV and get the accurate geographic information of the canal system or other ecological irrigation areas, thus providing a scientific reference for the management of precision irrigation.

Funding

This research was funded by the National Key R&D Program of China (Grant Nos. 2016YFC0400207, 2017YFD0701003

from 2017YFD0701000, and 2016YFD0200702 from 2016YFD0200700), the Jilin Province Key R&D Plan Project (Grant Nos. 20180201036SF and 20170204008SF), the Chinese Universities Scientific Fund (Grant Nos. 10710301, 1071-31051012,1071-31051361, and 2019TC108), Open Fund of Synergistic Innovation Center of Jiangsu Modern Agricultural Equipment and Technology, Jiangsu University (Grant No. 4091600002), and Open Fund of State Laboratory of Information Engineering in Surveying, Mapping and Remote Sensing, Wuhan University (Grant No. 19R06).

Acknowledgments

The corresponding author sincerely acknowledges the guidance of Prof. Hugh Hong-Tao Liu at University of Toronto Institute for Aerospace Studies (UTIAS).

References

[1] P.R. González, G.I. Fernández, M.M. Arroyo, D.J.A. Rodríguez, P.E. Camacho, P. Montesinos, Multi platform application for precision irrigation scheduling in strawberries, Agric. Water Manage., 183 (2017) 194–201.
[2] A.A. Anwar, W. Ahmad, M.T. Bhatti, Z.U. Haq, The potential of precision surface irrigation in the indus basin irrigation system, Irrigation Sci., 34 (2016) 379–396.
[3] I. Kisekka, T. Oker, G. Nguyen, J. Aguilar, D. Rogers, Revisiting precision mobile drip irrigation under limited water, Irrig. Sci., 35 (2017) 483–500.
[4] G. Egea, E.F. José, F. Alcon, Financial assessment of adopting irrigation technology for plant-based regulated deficit irrigation scheduling in super high-density olive orchards, Agric. Water Manage., 187 (2017) 47–56.
[5] L. Bai, J. Cai, Y. Liu, H. Chen, B. Zhang, L. Huang, Responses of field evapotranspiration to the changes of cropping pattern and groundwater depth in large irrigation district of yellow river basin, Agric. Water Manage., 188 (2017) 1–11.
[6] Q. Dong, Y.Z. Yang, T.B. Zhang, L.F. Zhou, J.Q. He, H.W. Chau, Y.F. Zou, H. Feng, Impacts of ridge with plastic mulch-furrow irrigation on soil salinity, spring maize yield and water use efficiency in an arid saline area, Agric. Water Manage., 201 (2017) 268–277.
[7] S. Kumar, M. Imtiyaz, A. Kumar, Studying the feasibility of using micro-irrigation systems for vegetable production in a canal command area, Irrig. Drainage, 58 (2010) 86–95.
[8] J. Xue, L. Ren, Assessing water productivity in the hetao irrigation district in inner mongolia by an agro-hydrological model, Irrig. Sci., 35 (2017) 257–382.
[9] Y.B. Wang, D. Liu, X.C. Cao, Z.Y. Yang, J.F. Song, D.Y. Chen, S.K. Sun, Agricultural water rights trading and virtual water export compensation coupling model: a case study of an irrigation district in china, Agric. Water Manage., 180 (2017) 99–106.
[10] X.Y. Gao, Y.N. Bai, Z.L. Huo, X. Xu, G.H. Huang, Y.H. Xia, T.S. Steenhuis, Deficit irrigation enhances contribution of shallow groundwater to crop water consumption in arid area, Agric. Water Manage., 185 (2017) 116–125.
[11] Z. Zhang, H. Guo, W. Zhao, S. Liu, Y. Cao, Y. Jia, Influences of groundwater extraction on flow dynamics and arsenic levels in the western Hetao basin, Inner Mongolia, China, Hydrogeology J., 26 (2018) 1–14.
[12] J. Vos, L. Vincent, Volumetric water control in a large-scale open canal irrigation system with many smallholders: the case of chancay-lambayeque in Peru, Agric. Water Manage., 98 (2011) 0–714.
[13] D. Delgoda, H. Malano, M.N. Halgamuge, S.K. Saleem, Novel generic optimization method for irrigation scheduling under multiple objectives and multiple hierarchical layers in a canal network, Adv. Water Resour., (2017) 105.
[14] D. Stroppiana, P. Villa, G. Sona, G. Ronchetti, G. Candiani, M. Pepe, L. Busetto, M. Migliazzi, M. Boschetti, Early season weed mapping in rice crops using multi–spectral UAV data, Int. J. Remote Sensing, 1 (2018) 1–21.
[15] R. Bhola, N.H. Krishna, K.N. Ramesh, J. Senthilnath, G. Anand, Detection of the power lines in UAV remote sensed images using spectral-spatial methods, J. Environ. Manage., 206 (2018) 1233.
[16] F. Li, W. Yang, X. Liu, G. Sun, J. Liu, Using high-resolution UAV-borne thermal infrared imagery to detect coal fires in Majiliang mine, Datong coalfield, northern China, Remote Sensing Lett., 9 (2018) 71–80.
[17] P. Surový, R.N. Almeida, D. Panagiotidis, Estimation of positions and heights from UAV-sensed imagery in tree plantations in agrosilvopastoral systems, Int. J. Remote Sensing, 1 (2018) 1–15.
[18] S.F.D. Gennaro, A. Matese, B. Gioli, P. Toscano, A. Zaldei, A. Palliotti, L. Genesio, Multi-sensor approach to assess vineyard thermal dynamics combining high-resolution unmanned aerial vehicle (UAV) remote sensing and wireless sensor network (WSN) proximal sensing, Scientia Horticulturae, 221 (2017) 83–87.
[19] J. Gago, C. Douthe, R.E. Coopman, P.P. Gallego, M. Ribas-Carbo, J. Flexas, J.M. Escalona, H. Medrano, UAVs challenge to assess water stress for sustainable agriculture, Agric. Water Manage., 153 (2015) 9–19.
[20] D.J. Mulla, Twenty five years of remote sensing in precision agriculture: key advances and remaining knowledge gaps, Biosyst. Eng., 114 (2013) 358–371.
[21] N. Bagheri, Development of a high-resolution aerial remote sensing system for precision agriculture, Int. J. Remote Sensing, 37 (2016) 1–13.
[22] J.F. Brown, M.S. Pervez, Merging remote sensing data and national agricultural statistics to model change in irrigated agriculture, Agric. Syst., 127 (2014) 28–40.
[23] W. Su, C. Zhang, J.Y. Yang, H.G. Wu, L. Deng, W.H. Ou, Y. Anzhi, M.J. Chen, Analysis of wavelet packet and statistical textures for object-oriented classification of forest-agriculture ecotones using SPOT 5 imagery, Int. J. Remote Sensing, 33 (2012) 23.
[24] B.R. Nikam, F. Ibragimov, A. Chouksey, V. Garg, S.P. Aggarwal, Retrieval of land surface temperature from Landsat 8 tirs for the command area of Mula irrigation project, Environ. Earth Sci., 75 (2016) 1169.
[25] Y. Huang, K.N. Reddy, R.S. Fletcher, D. Pennington, UAV low-altitude remote sensing for precision weed management, Weed Technol., 32 (2018) 1–5.
[26] H. Xiang, L. Tian, Method for automatic georeferencing aerial remote sensing (RS) images from an unmanned aerial vehicle (UAV) platform, Biosyst. Eng., 108 (2011) 104–113.
[27] M. Zhang, Low-level feature extraction for edge detection using genetic programming, IEEE Trans. Cybernetics, 44 (2017) 1459–1472.
[28] H. Yu, W. Yang, A fast feature extraction and matching algorithm for unmanned aerial vehicle images, J. Electron. Info. Technol., 38 (2016) 509–516.
[29] D. Liu, G. Hua, P. Viola, T. Chen, Integrated feature selection and higher-order spatial feature extraction for object categorization, Proc. IEEE Conference on Computer Vision and Pattern Recognition, 1 (2018) 1–8.
[30] Q. Wu, W. Diao, F. Dou, X. Sun, X. Zheng, K. Fu, Shape-based object extraction in high-resolution remote-sensing images using deep Boltzmann machine, Int. J. Remote Sensing, 37 (2016) 11.
[31] G. Gao, L. Zhou, Y. Li, A new change-detection method in high-resolution remote sensing images based on a conditional random field model, Int. J. Remote Sensing, 37 (2016) 17.
[32] S. Qiu, G. Wen, Z. Deng, J. Liu, Y. Fan, Accurate non-maximum suppression for object detection in high-resolution remote sensing images, Remote Sensing Lett., 37 (2016) 17.

[33] K. Parvathi, B.S.P. Rao, T.V. Rao, K.M. Reddy, Feature extraction from satellite images of hilly terrains using wavelets and watersheds, Int. J. Remote Sensing, 31 (2010) 12.
[34] L.J. Yang, Z. Tian, W. Zhao, A new affine invariant feature extraction method for sar image registration, Int. J. Remote Sensing, 35 (2014) 7219–7229.
[35] J. Li, Q. Hu, M. Ai, Unsupervised road extraction via a gaussian mixture model with object-based features, Int. J. Remote Sensing, 39 (2018) 2421–2440.
[36] E. Basaeed, H. Bhaskar, P. Hill, M. Al-Mualla, D.A. Bull, Supervised hierarchical segmentation of remote-sensing images using a committee of multi-scale convolutional neural networks, Int. J. Remote Sensing, 37 (2016) 21.
[37] J. Kang, L. Wang, F. Chen, Z. Niu, Identifying tree crown areas in undulating eucalyptus plantations using jseg multi-scale segmentation and unmanned aerial vehicle near-infrared imagery, Int. J. Remote Sensing, 38 (2017) 17.
[38] S. Chen, X. Li, L. Zhao, H. Yang, Medium-low resolution multi source remote sensing image registration based on sift and robust regional mutual information, Int. J. Remote Sensing, 39 (2018) 3215–3242.
[39] J. Liu, Scale computation on high spatial resolution remotely sensed imagery multi-scale segmentation, Int. J. Remote Sensing, 38 (2017) 5186–5214.
[40] S.E. Jozdani, M. Momeni, B.A. Johnson, M. Sattari, A regression modelling approach for optimizing segmentation scale parameters to extract buildings of different sizes, Int. J. Remote Sensing, 39 (2018) 684–703.
[41] F. Meng, X. Yang, C. Zhou, Z. Li, B. Liu, Multi scale adaptive reconstruction of missing information for remotely sensed data using sparse representation, Remote Sensing Lett., 9 (2018) 458–467.
[42] Z. Wang, C. Lu, X. Yang, Exponentially sampling scale parameters for the efficient segmentation of remote-sensing images, Int. J. Remote Sensing, 39 (2018) 1628–1654.
[43] A. Hadavand, M. Saadatseresht, S. Homayouni, Segmentation parameter selection for object-based land-cover mapping from ultra high resolution spectral and elevation data, Int. J. Remote Sensing, 38 (2017) 3586–3607.
[44] Y. Xu, W. Yao, L. Hoegner, U. Stilla, Segmentation of building roofs from airborne lidar point clouds using robust voxel-based region growing, Remote Sensing Lett., 8 (2017) 1062–1071.